Coherence effects in Mie scattering

Fischer, D.G.; van Dijk, T.; Visser, T.D.; Wolf, E.

published in
Journal of the Optical Society of America. A: Optics, image science, and vision.
2012

DOI (link to publisher)
10.1364/JOSAA.29.000078

document version
Publisher's PDF, also known as Version of record

Coherence effects in Mie scattering

David G. Fischer,[1,*] Thomas van Dijk,[2] Taco D. Visser,[2,3] and Emil Wolf[4]

[1]*Research and Technology Directorate, NASA Glenn Research Center, Cleveland, Ohio 44135, USA*
[2]*Department of Physics and Astronomy, Free University, Amsterdam, The Netherlands*
[3]*Department of Electrical Engineering, Delft University of Technology, Delft, The Netherlands*
[4]*Department of Physics and Astronomy, and The Institute of Optics, University of Rochester, Rochester, New York 14627, USA*
**Corresponding author: dgfischer@nasa.gov*

Received July 29, 2011; revised October 17, 2011; accepted October 20, 2011; posted October 20, 2011 (Doc. ID 151914); published December 7, 2011

The scattering of a partially coherent beam by a deterministic, spherical scatterer is studied. In particular, the Mie scattering by a Gaussian Schell-model beam is analyzed. Expressions are derived for (a) the extinguished power, (b) the radiant intensity of the scattered field, and (c) the encircled energy in the far field. It is found that the radiant intensity and the encircled energy in the far field depend on the degree of coherence of the incident beam, whereas the extinguished power does not. © 2012 Optical Society of America

OCIS codes: 030.1640, 290.4020, 290.5825.

1. INTRODUCTION

When considering the scattering of light by spherical particles (so-called Mie scattering), it is usually assumed that the incident field is spatially completely coherent [1–5]. However, in practice this assumption is not always justified. Examples of partially coherent fields include those generated by multimode lasers and beams that have passed through a random medium, e.g., the turbulent atmosphere. Such more general situations have only recently begun to attract attention [6–13].

In a previous study [12] the theory of Mie scattering has been generalized to include fields that are spatially partially coherent. In the present paper we use this formalism to study the scattering of partially coherent light (specifically, scattering of Gaussian Schell-model beams) by deterministic, spherical particles. In particular, we determine the influence of the degree of coherence of the incident beam on the total amount of scattered power (the extinction for nonabsorbing particles) and the angular distribution of the scattered power. We analyze the total scattered power and find that it is independent of the degree of coherence of the incident beam. This result agrees with one due to Greffet *et al.* [9]. We also investigate the angular intensity distribution of the scattered light (the radiant intensity). We find that the radiant intensity depends on the degree of coherence of the incident beam, most strongly when the effective transverse coherence width is comparable to the size of the scatterer. Finally, we calculate the encircled energy of the scattered radiation in the far zone of the scatterer for different detector geometries, as a function of the degree of coherence of the incident beam.

2. PARTIALLY COHERENT INCIDENT FIELD

We first consider a monochromatic, complex scalar wave field $V^{(i)}(\mathbf{r},t)$, which is incident on a spherical scatterer occupying a volume V. We represent the incident wave as

$$V^{(i)}(\mathbf{r},t)=U^{(i)}(\mathbf{r},\omega)\exp(-i\omega t). \tag{1}$$

Its time-independent part $U^{(i)}(\mathbf{r},\omega)$ may be represented in terms of its angular spectrum, i.e., as a superposition of plane-wave modes, each propagating along a direction specified by a unit vector $\mathbf{u}$ pointing into the half-space $z>0$, viz.

$$U^{(i)}(\mathbf{r},\omega)=\int_{|\mathbf{u}'_\perp|^2\le 1} a(\mathbf{u}'_\perp,\omega)e^{ik\mathbf{u}\cdot\mathbf{r}}\mathrm{d}^2u'_\perp. \tag{2}$$

Here $\mathbf{r}$ denotes the position vector of a point in space, t the time, ω the frequency, and $k=\omega/c$ is the wavenumber, c being the speed of light. Further, $\mathbf{u}'_\perp=(u'_x,u'_y)$ is the two-dimensional projection, considered a vector, of $\mathbf{u}$ onto the xy plane.

For a partially coherent wave field, one must consider, instead of the field $U^{(i)}(\mathbf{r},\omega)$, the *cross-spectral density function* of the field at a pair of points $\mathbf{r}_1$ and $\mathbf{r}_2$, namely (see Subsection 4.3.2 of [14])

$$W^{(i)}(\mathbf{r}_1,\mathbf{r}_2,\omega)=\langle U^{(i)*}(\mathbf{r}_1,\omega)U^{(i)}(\mathbf{r}_2,\omega)\rangle, \tag{3}$$

where the angular brackets represent the average over an ensemble of monochromatic realizations, all of frequency ω, of the incident field. On substituting from Eq. (2) into Eq. (3), we find that the cross-spectral density of the incident field is given by the expression

$$W^{(i)}(\mathbf{r}_1,\mathbf{r}_2,\omega)=\int_{|\mathbf{u}'_\perp|^2\le 1}\int_{|\mathbf{u}''_\perp|^2\le 1}\mathcal{A}(\mathbf{u}'_\perp,\mathbf{u}''_\perp,\omega)\times\exp[ik(\mathbf{u}''\cdot\mathbf{r}_2-\mathbf{u}'\cdot\mathbf{r}_1)]\mathrm{d}^2u'_\perp\mathrm{d}^2u''_\perp, \tag{4}$$

where

$$\mathcal{A}(\mathbf{u}'_\perp,\mathbf{u}''_\perp,\omega)=\langle a^*(\mathbf{u}'_\perp,\omega)a(\mathbf{u}''_\perp,\omega)\rangle \tag{5}$$

is the *angular correlation function* of the incident field (see Subsection 5.6.3 of [14]).

An important class of partially coherent fields, which includes the lowest-order Hermite–Gaussian laser mode, consists of the so-called *Gaussian Schell-model beams* (see Subsection 5.6.4 of [14]). The cross-spectral density function of such beams in the plane $z = 0$, which is taken to pass through the center O of the spherical scatter, may be expressed as

$$W^{(0)}(\boldsymbol{\rho}_1, \boldsymbol{\rho}_2, \omega) = [S^{(0)}(\boldsymbol{\rho}_1, \omega)]^{1/2}[S^{(0)}(\boldsymbol{\rho}_2, \omega)]^{1/2}\mu^{(0)}(\boldsymbol{\rho}_1 - \boldsymbol{\rho}_2, \omega), \tag{6}$$

where the spectral density, $S^{(0)}(\boldsymbol{\rho}, \omega)$, and the spectral degree of coherence, $\mu^{(0)}(\boldsymbol{\rho}_1 - \boldsymbol{\rho}_2, \omega)$, are both Gaussian functions, viz.

$$S^{(0)}(\boldsymbol{\rho}, \omega) = A_0^2 \exp(-\rho^2/2\sigma_S^2), \tag{7}$$

$$\mu^{(0)}(\boldsymbol{\rho}_1 - \boldsymbol{\rho}_2, \omega) = \exp[-(\rho_2 - \rho_1)^2/2\sigma_\mu^2]. \tag{8}$$

In these formulas $\boldsymbol{\rho} = (x, y)$ is a two-dimensional position vector of a point in the plane $z = 0$, and the positive parameters A_0, σ_S, and σ_μ are independent of position but may depend on frequency. We assume that the beam propagates in the positive z direction (see Fig. 1). It is evident from Eq. (4) that the angular correlation function of the beam is proportional to the inverse four-dimensional Fourier transform of the cross-spectral density, viz.

$$\mathcal{A}(\mathbf{u}'_\perp, \mathbf{u}''_\perp, \omega) = \left(\frac{k}{2\pi}\right)^4 \iiiint_{-\infty}^{+\infty} W^{(0)}(\boldsymbol{\rho}_1, \boldsymbol{\rho}_2, \omega) \times \exp[-ik(\mathbf{u}''_\perp \cdot \boldsymbol{\rho}_2 - \mathbf{u}'_\perp \cdot \boldsymbol{\rho}_1)]\mathrm{d}^2\rho_1 \mathrm{d}^2\rho_2. \tag{9}$$

On substituting from Eq. (6) into Eq. (9) and making the change of variables

$$\mathbf{U} = \boldsymbol{\rho}_2 - \boldsymbol{\rho}_1, \tag{10}$$

$$\mathbf{V} = (\boldsymbol{\rho}_1 + \boldsymbol{\rho}_2)/2, \tag{11}$$

one obtains for the angular correlation function the expression

$$\mathcal{A}(\mathbf{u}'_\perp, \mathbf{u}''_\perp, \omega) = \left(\frac{k^2 A_0 \sigma_S \sigma_{\mathrm{eff}}}{2\pi}\right)^2 \times \exp\left\{-\frac{k^2}{2}\left[(\mathbf{u}'_\perp - \mathbf{u}''_\perp)^2\sigma_S^2 + (\mathbf{u}'_\perp + \mathbf{u}''_\perp)^2\frac{\sigma_{\mathrm{eff}}^2}{4}\right]\right\}, \tag{12}$$

where

$$\frac{1}{\sigma_{\mathrm{eff}}^2} = \frac{1}{\sigma_\mu^2} + \frac{1}{4\sigma_S^2}. \tag{13}$$

In order for the field to be beamlike, the parameters σ_S and σ_μ must satisfy the relation {Eq. (5.6-73) of [14]}

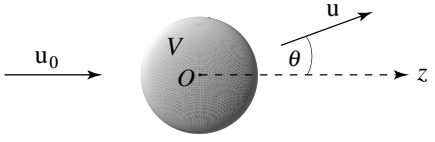

Fig. 1. Illustrating the notation.

$$\frac{1}{\sigma_\mu^2} + \frac{1}{4\sigma_S^2} \ll \frac{k^2}{2}. \tag{14}$$

We will use Eq. (12) in the analysis of scattering of a Gaussian Schell-model beam by a sphere.

In the analysis of scattering phenomena, one usually normalizes the scattered power by that of the incident field. It seems therefore natural to ask the question whether the power carried by a partially coherent beam is independent of its degree of coherence. If this is the case, then the effect of the degree of coherence on the scattering phenomena can be isolated, and, indeed, we find this is so for scattering of Gaussian Schell-model beams. A proof is presented in Appendix A.

3. SCATTERED FIELD

A. Angular Dependence of the Intensity of the Scattered Field

When a monochromatic plane wave is incident on a scatterer in the direction of a unit vector $\mathbf{u}_0$, the scattered field in the far zone at the point $\mathbf{r} = r\mathbf{u}$, with $|\mathbf{u} = 1|$, has the form

$$U^{(s)}(r\mathbf{u}, \omega) \sim f(\mathbf{u}, \mathbf{u}_0, \omega)\frac{e^{ikr}}{r}, \qquad (kr \to \infty, \mathbf{u}\ \text{fixed}), \tag{15}$$

where $f(\mathbf{u}, \mathbf{u}_0, \omega)$ is the *scattering amplitude*. When the incident field is not a plane wave but rather is given by a superposition of plane waves as expressed by Eq. (2), one has, instead of Eq. (15), the more general expression

$$U^{(s)}(r\mathbf{u}, \omega) \sim \frac{e^{ikr}}{r}\int_{|\mathbf{u}'_\perp|^2 \le 1} a(\mathbf{u}'_\perp, \omega) f(\mathbf{u}, \mathbf{u}', \omega)\mathrm{d}^2 u'_\perp. \tag{16}$$

A central quantity that describes the behavior of the scattered field in the far zone is its *radiant intensity* $J^{(s)}(\mathbf{u}, \omega)$, given by the expression (see Subsection 5.2 of [14])

$$J^{(s)}(\mathbf{u}, \omega) = r^2\langle U^{(s)*}(r\mathbf{u}, \omega)U^{(s)}(r\mathbf{u}, \omega)\rangle, \times (kr \to \infty, \text{with}\ \mathbf{u}\ \text{fixed}). \tag{17}$$

On substituting from Eq. (16) into Eq. (17), we find that the radiant intensity of the scattered field is given by the formula

$$J^{(s)}(\mathbf{u}, \omega) = \iint \mathcal{A}(\mathbf{u}'_\perp, \mathbf{u}''_\perp, \omega) f^*(\mathbf{u}, \mathbf{u}', \omega) f(\mathbf{u}, \mathbf{u}'', \omega)\mathrm{d}^2 u'_\perp \mathrm{d}^2 u''_\perp. \tag{18}$$

On making use in Eq. (18) of Eq. (12) for the angular correlation function of a Gaussian Schell-model beam, the expression for the radiant intensity takes on the form

$$J^{(s)}(\mathbf{u}, \omega) = \left(\frac{k^2 A_0 \sigma_S \sigma_{\mathrm{eff}}}{2\pi}\right)^2 \times \iint \exp\left\{-\frac{k^2}{2}\left[(\mathbf{u}'_\perp - \mathbf{u}''_\perp)^2\sigma_S^2 + (\mathbf{u}'_\perp + \mathbf{u}''_\perp)^2\frac{\sigma_{\mathrm{eff}}^2}{4}\right]\right\} \times f^*(\mathbf{u}, \mathbf{u}', \omega) f(\mathbf{u}, \mathbf{u}'', \omega)\mathrm{d}^2 u'_\perp \mathrm{d}^2 u''_\perp. \tag{19}$$

We take the axis of the incident beam to pass through the center of the spherical scatterer. The scattering amplitude then has the form

$$f(\mathbf{u}',\mathbf{u}'',\omega)=f(\mathbf{u}'\cdot\mathbf{u}'',\omega)=f(\theta,\omega), \tag{20}$$

i.e., it depends only on the angle θ between the direction of incidence $\mathbf{u}''$ and the direction of scattering $\mathbf{u}'$ (see Fig. 1). For a spherical scatterer of radius a, with refractive index n, the scattering amplitude can be expressed in terms of the phase shifts $\delta_l(\omega)$ as {see Eq. (4.66) of [15]}

$$f(\theta,\omega)=\frac{1}{k}\sum_{l=0}^{\infty}(2l+1)\exp[i\delta_l(\omega)]\sin\delta_l(\omega)P_l(\cos\theta). \tag{21}$$

Here P_l denotes a Legendre polynomial, and the phase shifts $\delta_l(\omega)$ are given by the expressions (see Subsections 4.3.2 and 4.4.1 of [15])

$$\tan\delta_l(\omega)=\frac{\bar{k}j_l(ka)j_l'(\bar{k}a)-kj_l(\bar{k}a)j_l'(ka)}{\bar{k}j_l'(\bar{k}a)n_l(ka)-kj_l(\bar{k}a)n_l'(ka)}, \tag{22}$$

where j_l denotes the spherical Bessel function of order l and n_l denotes the spherical Neumann function of the same order. Further,

$$\bar{k}=nk, \tag{23}$$

$$j_l'(ka)=\left.\frac{dj_l(x)}{dx}\right|_{x=ka}, \tag{24}$$

$$n_l'(ka)=\left.\frac{dn_l(x)}{dx}\right|_{x=ka}. \tag{25}$$

If we substitute from Eq. (21) for the scattering potential into Eq. (19), we obtain for the radiant intensity the expression

$$J^{(s)}(\mathbf{u},\omega)=\left(\frac{kA_0\sigma_S\sigma_{\mathrm{eff}}}{2\pi}\right)^2\sum_{l=0}^{\infty}\sum_{m=0}^{\infty}b_l^*(\omega)b_m(\omega)\times\iint\exp\left\{-\frac{k^2}{2}\left[(\mathbf{u}_\perp'-\mathbf{u}_\perp'')^2\sigma_S^2+(\mathbf{u}_\perp'+\mathbf{u}_\perp'')^2\frac{\sigma_{\mathrm{eff}}^2}{4}\right]\right\}\times P_l(\mathbf{u}\cdot\mathbf{u}')P_m(\mathbf{u}\cdot\mathbf{u}'')\mathrm{d}^2u_\perp'\,\mathrm{d}^2u_\perp'', \tag{26}$$

where, for brevity, we have written

$$b_m(\omega)=(2m+1)\exp[i\delta_m(\omega)]\sin\delta_m(\omega). \tag{27}$$

We will restrict ourselves to the case where the beam width is much greater than its transverse coherence length, i.e., $\sigma_S\gg\sigma_\mu$. Under these circumstances one can obtain an asymptotic approximation as $k\sigma_S\to\infty$ for the double integral over $\mathbf{u}_\perp''$ using Laplace's method [16]. This method asserts that, for two well-behaved functions $f(x,y)$ and $g(x,y)$ defined over a two-dimensional domain D,

$$\iint_D e^{-pf(x,y)}g(x,y)\mathrm{d}x\mathrm{d}y\approx\frac{2\pi g(x_0,y_0)}{p\sqrt{\mathrm{Det}\{H[f(x_0,y_0)]\}}}e^{-pf(x_0,y_0)},\quad\text{as } p\to\infty, \tag{28}$$

where (x_0,y_0) is the point at which $f(x,y)$ has a minimum. Further, $H[f(x_0,y_0)]$ is the Hessian matrix of $f(x,y)$ evaluated at (x_0,y_0), i.e.,

$$H[f(x_0,y_0)]=\left.\begin{pmatrix}\frac{\partial^2f(x,y)}{\partial x^2} & \frac{\partial^2f(x,y)}{\partial x\partial y}\\ \frac{\partial^2f(x,y)}{\partial y\partial x} & \frac{\partial^2f(x,y)}{\partial y^2}\end{pmatrix}\right|_{x_0,y_0}.$$

We make use of Eq. (28) with the choices

$$g(\mathbf{u},\mathbf{u}_\perp',\mathbf{u}_\perp'')=\left(\frac{kA_0\sigma_S\sigma_{\mathrm{eff}}}{2\pi}\right)^2\sum_{l=0}^{\infty}\sum_{m=0}^{\infty}b_l^*(\omega)b_m(\omega)P_l(\mathbf{u}\cdot\mathbf{u}')\times P_m(\mathbf{u}\cdot\mathbf{u}'')\exp\left\{-\frac{k^2\sigma_{\mathrm{eff}}^2}{8}(\mathbf{u}_\perp'+\mathbf{u}_\perp'')^2\right\}, \tag{29}$$

$$f(\mathbf{u}_\perp',\mathbf{u}_\perp'')=\frac{1}{2}(\mathbf{u}_\perp'-\mathbf{u}_\perp'')^2, \tag{30}$$

$$p=(k\sigma_S)^2. \tag{31}$$

The minimum of the function of $\mathbf{u}_\perp''$ occurs when $u_x''=u_x'$ and $u_y''=u_y'$, and the determinant of the Hessian matrix, evaluated at this point, can be shown to have the value unity. Equation (26) for the radiant intensity then reduces to

$$J^{(s)}(\mathbf{u},\omega)=\frac{A_0^2\sigma_\mu^2}{2\pi}\sum_{l=0}^{\infty}\sum_{m=0}^{\infty}b_l^*(\omega)b_m(\omega)\times\int P_l(\mathbf{u}\cdot\mathbf{u}')P_m(\mathbf{u}\cdot\mathbf{u}')e^{-k^2\sigma_\mu^2u_\perp'^2/2}\mathrm{d}^2u_\perp'. \tag{32}$$

or, written more explicitly,

$$J^{(s)}(\mathbf{u},\omega)=\frac{A_0^2\sigma_\mu^2}{2\pi}\sum_{l=0}^{\infty}\sum_{m=0}^{\infty}(2l+1)(2m+1)e^{i(\delta_l-\delta_m)}\sin\delta_l\sin\delta_m\times\int_{|\mathbf{u}_\perp'|^2\le1}P_l(\mathbf{u}\cdot\mathbf{u}')P_m(\mathbf{u}\cdot\mathbf{u}')e^{-k^2\sigma_\mu^2u_\perp'^2/2}\mathrm{d}^2u_\perp', \tag{33}$$

where we have used the fact that $\sigma_{\mathrm{eff}}\to\sigma_\mu$ as $\sigma_S\to\infty$. By symmetry, the radiant intensity depends only on the angle θ between the beam axis (the z axis) and the direction of scattering.

Several examples of the angular distribution of the radiation generated by scattering from spheres of different radii, calculated from Eq. (33), are shown in Figs. 2–4. Two trends can clearly be distinguished. As the size of the scatterer increases, the field becomes more strongly peaked in the forward direction and there are more oscillations in the scattering pattern. Also, as the transverse coherence length σ_μ decreases, the radiant intensity becomes more isotropic. In particular, this is seen to occur when the coherence length is comparable to the size of the scatterer. This is in agreement with experimental observations reported by Gori *et al.* [17].

In Fig. 5 the radiant intensity, plotted as a function of the scattering angle, is shown on a logarithmic scale, illustrating more clearly its fine structure. It is seen that, as σ_μ decreases, the characteristic deep minima gradually disappear and the radiation pattern becomes smoothed out.

B. Total Scattered Power

The total scattered power $P^{(s)}(\sigma_\mu,\omega)$ is given by the integral of the radiant intensity over all directions (see Subsection 5.7 of [14]), i.e.,

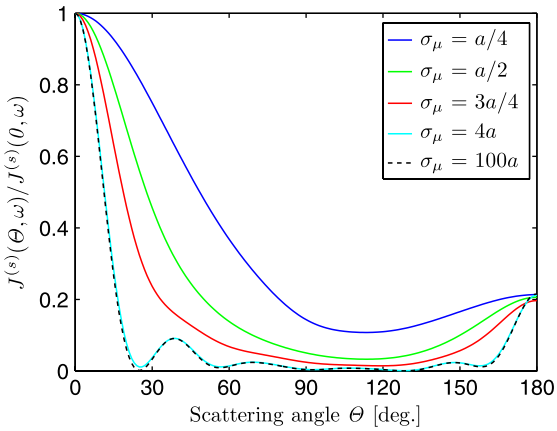

Fig. 2. (Color online) Normalized angular distribution of the radiant intensity generated by scattering a partially coherent beam by a sphere, for various values of the transverse coherence length σ_μ. In this example, the sphere radius $a = 1\lambda$, and the refractive index $n = 2$.

$$P^{(s)}(\sigma_\mu,\omega) = \int_{(4\pi)} J^{(s)}(\mathbf{u},\omega)\mathrm{d}\Omega. \tag{34}$$

On substituting from Eq. (33) into Eq. (34), we find that

$$P^{(s)}(\sigma_\mu,\omega) = 2A_0^2\sigma_\mu^2\sum_{l=0}^{\infty}(2l+1)\sin^2\delta_l\int_{|\mathbf{u}'_\perp|^2\le 1} e^{-k^2\sigma_\mu^2 u'^2_\perp/2}\mathrm{d}^2u'_\perp, \tag{35}$$

where we have used the identity [18]

$$\int_{(4\pi)} P_l(\mathbf{u}\cdot\mathbf{u}')P_m(\mathbf{u}\cdot\mathbf{u}')\mathrm{d}\Omega = \frac{4\pi}{2l+1}\delta_{lm}. \tag{36}$$

If we now express $\mathbf{u}'$ in component form, i.e., $\mathbf{u}' = (\cos\phi'\sin\theta', \sin\phi'\sin\theta', \cos\theta')$, we obtain the formulas

$$\begin{aligned} P^{(s)}(\sigma_\mu,\omega) &= 4\pi A_0^2\sigma_\mu^2\sum_{l=0}^{\infty}(2l+1)\frac{\tan^2\delta_l}{1+\tan^2\delta_l}\int_0^{\pi/2} \\ &\quad\times\exp[-k^2\sigma_\mu^2\sin^2\theta'/2]\sin\theta'\cos\theta'\mathrm{d}\theta' \\ &= \frac{4\pi A_0^2}{k^2}\sum_{l=0}^{\infty}(2l+1)\frac{\tan^2\delta_l}{1+\tan^2\delta_l}\left[1-\exp\left(\frac{-k^2\sigma_\mu^2}{2}\right)\right]. \end{aligned} \tag{37}$$

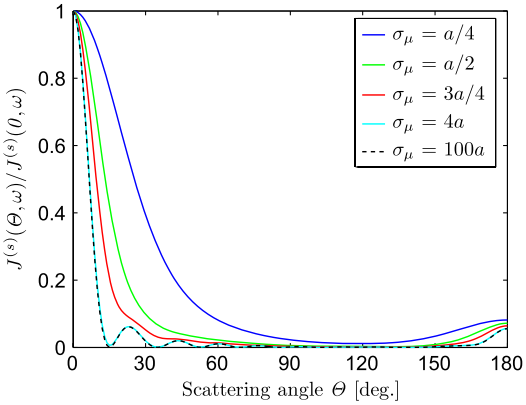

Fig. 3. (Color online) Normalized angular distribution of the radiant intensity generated by scattering a partially coherent beam by a sphere, for various values of the transverse coherence length σ_μ. In this example, the sphere radius $a = 2\lambda$, and the refractive index $n = 2$.

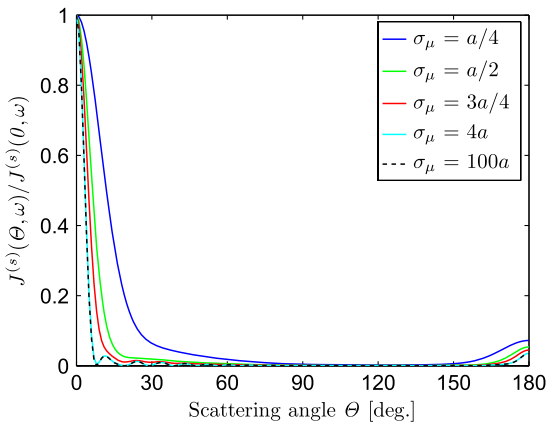

Fig. 4. (Color online) Normalized angular distribution of the radiant intensity generated by scattering a partially coherent beam by a sphere, for various values of the transverse coherence length σ_μ. In this example, the sphere radius $a = 4\lambda$, and the refractive index $n = 2$.

In the case that we are considering, namely that of a beam with a width that is much greater than the transverse coherence length, i.e., when $\sigma_S \gg \sigma_\mu$, we have from Eq. (13) that $\sigma_{\mathrm{eff}} \approx \sigma_\mu$. The beam condition Eq. (14) then becomes $k^2\sigma_\mu^2 \gg 2$. It is seen that Eq. (37) now reduces to the *optical theorem* for the absorption-free case (see Subsection 13.3 of [3]), i.e.,

$$P^{(e)}(\omega) = \frac{4\pi A_0^2}{k}\mathfrak{F}f(\mathbf{u}_0,\mathbf{u}_0), \tag{38}$$

where $P^{(e)}(\omega)$ denotes the extinguished power and $\mathfrak{F}$ the imaginary part. Hence, we conclude that, for Gaussian Schell-model beams whose effective width is much greater than their transverse coherence length, which are scattered from a sphere, the total amount of scattered power is independent of their state of coherence.

C. Power Intercepted by a Finite Detector

Apart from the total scattered power, power measurements with a finite-sized detector situated in the far zone are also of practical interest. The power captured by a detector centered on the z axis and subtending a half-angle θ_D at the origin O (see Fig. 1), is given by the expression

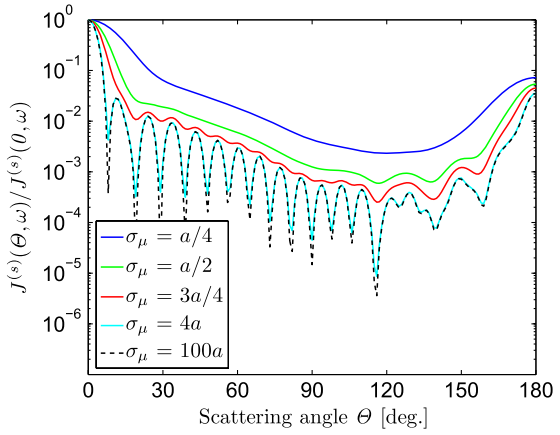

Fig. 5. (Color online) Normalized angular distribution of the radiant intensity generated by scattering a partially coherent beam by a sphere, shown on a logarithmic scale, for various values of the transverse coherence length σ_μ. In this example, the sphere radius $a = 4\lambda$, and the refractive index $n = 2$.

$$P^{(s)}(\theta_D,\sigma_\mu,\omega)=\frac{\int_{(\Omega_D)}J^{(s)}(\mathbf{u},\omega)\mathrm{d}\Omega}{\int_{(4\pi)}J^{(s)}(\mathbf{u},\omega)\mathrm{d}\Omega}=\frac{\int_0^{\theta_D}J^{(s)}(\theta,\omega)\sin\theta\mathrm{d}\theta}{\int_0^{\pi}J^{(s)}(\theta,\omega)\sin\theta\mathrm{d}\theta}. \tag{39}$$

Several examples of the detected power as a function of the angle subtended by the detector at the origin are presented in Figs. 6–8.

We see that, when the incident beam is fairly incoherent ($\sigma_\mu \le a$) and the scattering is more or less isotropic, the intercepted power essentially increases linearly with the detector's subtense, up to the extent of the scattering pattern. When the incident field is more coherent and the scattered power is spread nonuniformly in angle (i.e., the field has fine structure or oscillations), the intercepted power has a nonlinear dependence on the detector subtense. As the detector subtense is increased, the intercepted power can rise sharply or not much at all. This behavior is particularly pronounced for larger spheres.

In addition, especially for smaller spheres, the intercepted power for a particular detector subtense increases with increasing transverse coherence length. For larger spheres, however, there are cases when the intercepted power for a partially coherent incident field may be greater than that for a field that is more coherent. This is seen in Figs. 7 and 8 where the curve for the more coherent case ($\sigma_\mu = 4a$) dips below that for the less coherent ones.

The interplay between angular subtense of the detector and the state of coherence of the incident beam can also be visualized by examining the scattered power for fixed detector size, as a function of the coherence length σ_μ (see Figs. 9–11). It is seen that the measured power typically saturates when σ_μ becomes sufficiently large. This saturation occurs for larger values of σ_μ when the subtended angle θ_D is smaller. In addition, this anomalous behavior of the detected power decreasing with increasing transverse coherence can be seen in Fig. 10 for $\theta_D = 18°$.

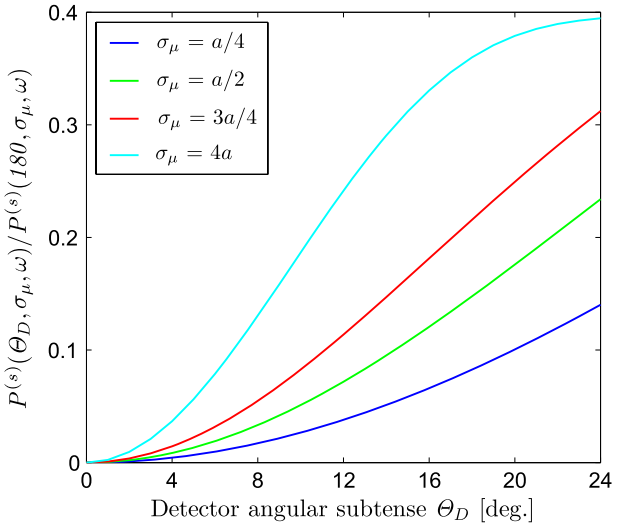

Fig. 6. (Color online) Normalized intercepted power as a function of the angle subtended by the detector for various values of the transverse coherence length σ_μ. In this example, the sphere radius $a = 1\lambda$, and the refractive index $n = 2$.

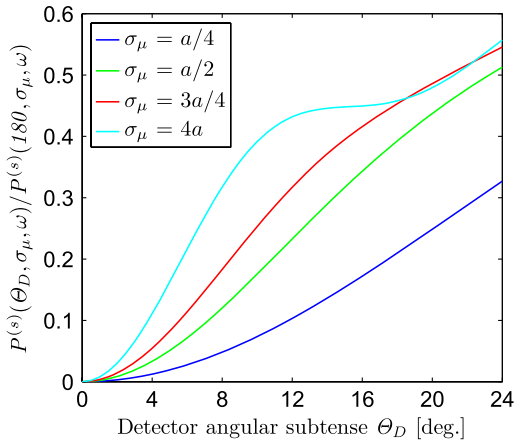

Fig. 7. (Color online) Normalized intercepted power as a function of the angle subtended by the detector for various values of the transverse coherence length σ_μ. In this example, the sphere radius $a = 2\lambda$, and the refractive index $n = 2$.

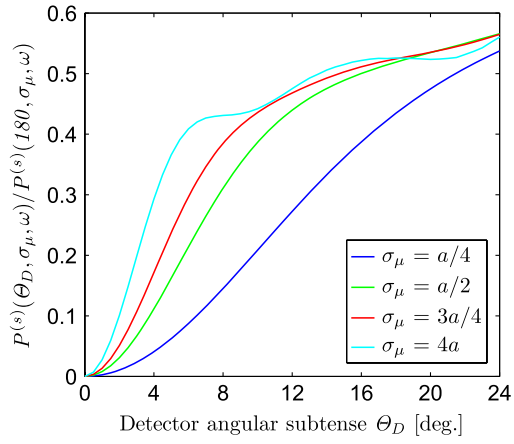

Fig. 8. (Color online) Normalized intercepted power as a function of the angle subtended by the detector for various values of the transverse coherence length σ_μ. In this example, the sphere radius $a = 4\lambda$, and the refractive index $n = 2$.

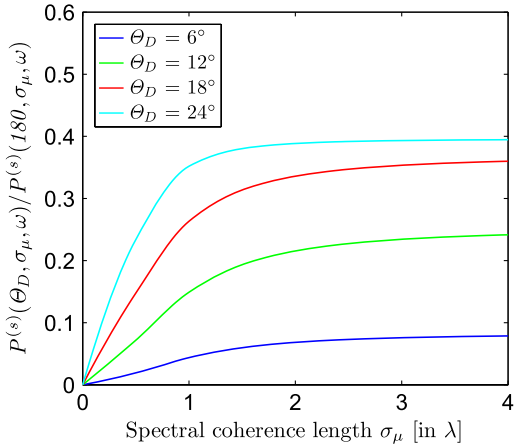

Fig. 9. (Color online) Normalized intercepted power as a function of the transverse coherence length σ_μ for several values of the angle subtended by the detector. In this example, the sphere radius $a = 1\lambda$, and the refractive index $n = 2$.

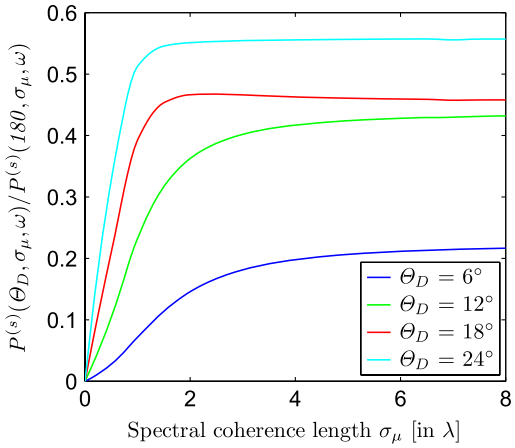

Fig. 10. (Color online) Normalized intercepted power as a function of the transverse coherence length σ_μ for several values of the angle subtended by the detector. In this example, the sphere radius $a = 2\lambda$, and the refractive index $n = 2$.

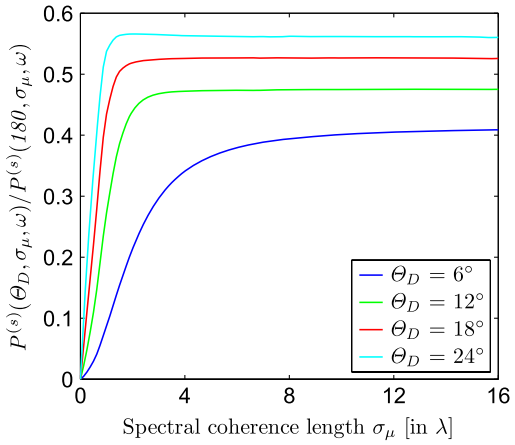

Fig. 11. (Color online) Normalized intercepted power as a function of the transverse coherence length σ_μ for several values of the angle subtended by the detector. In this example, the sphere radius $a = 4\lambda$, and the refractive index $n = 2$.

4. CONCLUSIONS

We have examined the effects of the state of spatial coherence of an incident beam on the scattering by a deterministic, spherical scatterer. The beams were assumed to be of the Gaussian Schell-model type. The total scattered power was shown to be independent of their state of coherence. However, the angular distribution of the scattered field was found to depend strongly on the state of coherence of the beam, especially when the transverse coherence length is comparable to the size of the scattering sphere. The power intercepted by a finite-sized detector was shown to vary significantly under such conditions. These results may be of importance, for example, in Mie scattering in the atmosphere and in scattering from colloidal suspensions.

APPENDIX A: POWER CONTENT OF GAUSSIAN SCHELL-MODEL BEAMS

In this Appendix we establish a property of Gaussian Schell-model beams that does not appear to have been noted before. The radiant intensity $J^{(i)}(\mathbf{u},\omega)$ of the beam in the direction $\mathbf{u} = (\cos\phi\sin\theta, \sin\phi\sin\theta, \cos\theta)$ can be expressed in terms of its angular correlation function $\mathcal{A}(\mathbf{u}'_\perp, \mathbf{u}''_\perp, \omega)$ {see Eq. (5.6-53) of [14]} by the formula

$$J^{(i)}(\mathbf{u},\omega) = \left(\frac{2\pi}{k}\right)^2 \mathcal{A}(\mathbf{u}_\perp, \mathbf{u}_\perp, \omega)\cos^2\theta, \tag{A1}$$

$$= (A_0 k\sigma_S\sigma_{\text{eff}})^2 \cos^2\theta \exp[-k^2\sigma_{\text{eff}}^2 \sin^2(\theta)/2], \tag{A2}$$

where Eq. (12), together with the expression $\mathbf{u}_\perp^2 = \sin^2\theta$, was used. The total power $P(\sigma_S,\sigma_\mu,\omega)$ that is carried by the beam is given by the integral of the radiant intensity over a hemisphere at infinity in the half-space $z > 0$, i.e.,

$$P(\sigma_S,\sigma_\mu,\omega) = \int_{(2\pi)} J^{(i)}(\mathbf{u},\omega)\mathrm{d}\Omega, \tag{A3}$$

with $d\Omega = \sin\theta d\theta d\phi$ being the element of solid angle. On substituting from Eq. (A2) into Eq. (A3), we obtain for the total power the expression

$$P(\sigma_S,\sigma_\mu,\omega) = 2\pi(A_0 k\sigma_S\sigma_{\text{eff}})^2 \times \int_0^{\pi/2} \exp[-k^2\sigma_{\text{eff}}^2 \sin^2(\theta)/2]\cos^2\theta\sin\theta\mathrm{d}\theta, \tag{A4}$$

$$= 2\pi A_0^2\sigma_S^2\left[1 - \frac{\exp(-k^2\sigma_{\text{eff}}^2/2)\sqrt{\pi/2}\,\text{erfi}\left(k\sigma_{\text{eff}}/\sqrt{2}\right)}{k\sigma_{\text{eff}}}\right], \tag{A5}$$

where $\text{erfi}(x) = \text{erf}(ix)/i$ denotes the error function with imaginary argument, erf being the ordinary error function, i.e.,

$$\text{erf}(x) = \frac{2}{\sqrt{\pi}}\int_0^x \exp(-t^2)\mathrm{d}t. \tag{A6}$$

The dependence on the state of coherence of the total power that is carried by the beam is contained in the factor σ_{eff} that appears in Eq. (A5). The beam condition, Eq. (14), can be expressed as $k\sigma_{\text{eff}} \gg 2^{1/2}$. Under that condition the second term within brackets of Eq. (A5) is negligible compared to unity, and the formula for the total beam power reduces to

$$P(\sigma_S,\omega) = 2\pi A_0^2\sigma_S^2, \qquad (k\sigma_{\text{eff}} \gg 2^{1/2}). \tag{A7}$$

We have written $P(\sigma_S,\omega)$ rather than $P(\sigma_S,\sigma_\mu,\omega)$ since, according to Eq. (A7), the power that is carried by a Gaussian Schell-model beam is independent of the coherence length σ_μ.

We conclude that Gaussian Schell-model beams with the same transverse intensity profile but with different states of coherence carry the same amount of power, namely that of a fully coherent beam ($\sigma_\mu \to \infty$). We note that Eq. (A7) can also be obtained by integration of the spectral density over the plane $z = 0$. However, for non-beamlike partially coherent fields, this may not be the case (see [19]).

ACKNOWLEDGMENTS

The research of E. W. is supported by the United States Air Force Office of Scientific Research (USAFOSR) under grant FA9550-08-1-0417. T. D. V. acknowledges support from The

Netherlands Foundation for Fundamental Research of Matter (FOM).

REFERENCES

1. G. Mie, "Beiträge zur Optik trüber Medien, speziell kolloidaler Metallösungen," Ann. Phys. **IV**, Folge 25, 377–445 (1908).
2. H. C. van de Hulst, *Light Scattering by Small Particles* (Wiley, 1957). See Chap. 9.
3. M. Born and E. Wolf, *Principles of Optics*, 7th (expanded) ed. (Cambridge University, 1999).
4. H. M. Nussenzveig, *Diffraction Effects in Semiclassical Scattering* (Cambridge University, 1992). See Chap. 5.
5. W. T. Grandy, Jr., *Scattering of Waves from Large Spheres* (Cambridge University, 1992). See Chap. 3.
6. P. S. Carney, E. Wolf, and G. S. Agarwal, "Statistical generalizations of the optical cross-section theorem with application to inverse scattering," J. Opt. Soc. Am. A **14**, 3366–3371 (1997).
7. P. S. Carney and E. Wolf, "An energy theorem for scattering of partially coherent beams," Opt. Commun. **155**, 1–6 (1998).
8. D. Cabaret, S. Rossano, and C. Brouder, "Mie scattering of a partially coherent beam," Opt. Commun. **150**, 239–250 (1998).
9. J. J. Greffet, M. De La Cruz-Gutierrez, P. V. Ignatovich, and A. Radunsky, "Influence of spatial coherence on scattering by a particle," J. Opt. Soc. Am. A **20**, 2315–2320 (2003).
10. T. D. Visser, D. G. Fischer, and E. Wolf, "Scattering of light from quasi-homogeneous sources by quasi-homogeneous media," J. Opt. Soc. Am. A **23**, 1631–1638 (2006).
11. E. Wolf, *Introduction to the Theory of Coherence and Polarization of Light* (Cambridge University, 2007). See Chap. 6.
12. T. van Dijk, D. G. Fischer, T. D. Visser, and E. Wolf, "Effects of spatial coherence on the angular distribution of radiant intensity generated by scattering on a sphere," Phys. Rev. Lett. **104**, 173902 (2010).
13. G. Gbur and T. D. Visser, "The structure of partially coherent fields," in Vol. 55 of *Progress in Optics*, E. Wolf, ed. (Elsevier, 2010), pp. 285–341.
14. L. Mandel and E. Wolf, *Optical Coherence and Quantum Optics* (Cambridge University, 1995).
15. C. J. Joachain, *Quantum Collision Theory*, 3rd ed. (Elsevier, 1987).
16. D. Zwillinger, *Handbook of Integration* (Jones and Bartlett, 1992), Chap. 8.
17. F. Gori, C. Palma, and M. Santarsiero, "A scattering experiment with partially coherent light," Opt. Commun. **74**, 353–356 (1990).
18. G. A. Korn and T. M. Korn, *Mathematical Handbook for Scientists and Engineers*, 2nd ed. (McGraw, 1968). See p. 852.
19. M. W. Kowarz and E. Wolf, "Conservation laws for partially coherent free fields," J. Opt. Soc. Am. A **10**, 88–94 (1993).